

Effect of Deprotection Extent on Swelling and Dissolution Regimes of Thin Polymer Films

Ashwin Rao, Shuhui Kang, Bryan D. Vogt,[†] Vivek M. Prabhu,* Eric K. Lin, Wen-Li Wu, and M. Muthukumar[‡]

Polymers Division, National Institute of Standards and Technology, Gaithersburg, Maryland 20899, and Department of Polymer Science and Engineering, University of Massachusetts, Amherst, Massachusetts 01003

Received June 20, 2006. In Final Form: September 11, 2006

The response of unentangled polymer thin films to aqueous hydroxide solutions is measured as a function of increasing weakly acidic methacrylic acid comonomer content produced by an in situ reaction–diffusion process. Quartz crystal microbalance with energy dissipation and Fourier transform infrared spectroscopy measurements are used to identify four regimes: (I) nonswelling, (II) quasiequilibrium swelling, (III) swelling coupled with partial film dissolution, and (IV) film dissolution. These regimes result from chemical heterogeneity in local composition of the polymer film. The acid-catalyzed deprotection of a hydrophobic group to the methacrylic acid tends to increase the hydrophilic domain size within the film. This nanoscale structure swells in aqueous base by ionization of the methacrylic acid groups. The swollen film stability, however, is determined by the hydrophobic matrix that can act as physical cross-links to prevent dissolution of the polyelectrolyte chains. These observations challenge current models of photoresist film dissolution that do not include the effects of swelling and partial film dissolution on image quality.

I. Introduction

The microlithography industry has successfully developed new materials to image sub-45-nm features through systematic changes in the chemistry and composition of the polymeric photoresist materials.¹ Resolving these structures depends on the change in polymer solubility over a narrow range of chemical composition that is controlled through a chemical reaction during the imaging process. This change in film composition is produced by an acid-catalyzed deprotection reaction that converts hydrophobic groups to weakly acidic groups. As the concentration of acidic groups increases, the polymer becomes soluble in an aqueous hydroxide solution (developer). One key element in the design of new photoresist polymer materials is controlling the ionization of the polymer during the dissolution process.

Numerous approaches have been taken to understand photoresist polymer dissolution through the application of percolation models,^{2–4} the investigation of interfacial reaction kinetics,⁵ the development of a surface-etching critical ionization model,^{6,7} and the combination of reaction kinetics with a critical ionization model.^{8,9} These studies focused on the kinetics of the dissolution process and have highlighted the influence of the polymer molecular weight and developer pH, especially with regard to

correlations to surface roughening. These models and experiments were developed primarily for a previous generation of photoresist materials that did not swell during development but dissolved in a manner similar to an etching process. However, many ionizable polymers can swell when exposed to an aqueous solution.⁸ For these classes of photoresist polymers, the effect of swelling on the rate of dissolution and the influence of the polymer chemistry on swelling remain poorly characterized; swelling may occur for polymers below the entanglement molecular weight and in the absence of chemical cross-links.^{10–13} These swollen film can be stable over long times, suggesting the presence of a restoring force that limits the swelling and inhibits dissolution. In this case, the solvent permeates the entire film and swelling is coupled to the chain ionization.^{8,12} To suppress swelling, additives and inert comonomers¹³ are often incorporated into these photoresist formulations. However, this can also lead to problems in other aspects of resist design, such as transparency and sensitivity.

In this work, we investigate the response of a thin film to an aqueous base solution as a function of the average composition of the polymer as it changes during an acid-catalyzed deprotection reaction. The photoacid reaction–diffusion process used in modern photolithography produces a chemically heterogeneous thin film.^{9,14–18} In this process, a photoacid is generated by light exposure from an initial random distribution of photoacid

* Corresponding author. Fax: (301) 975-3928. E-mail: vprabhu@nist.gov.

[†] Present address: Department of Chemical Engineering, Arizona State University, Tempe, AZ 85287.

[‡] University of Massachusetts.

- (1) Ito, H. *Adv. Polym. Sci.* **2005**, *172*, 37–245.
- (2) Oertel, H. K.; Weiss, M.; Dammel, R.; Theis, J. *Microelectron. Eng.* **1990**, *11* (1–4), 267–270.
- (3) Yeh, T. F.; Shih, H. Y.; Reiser, A. *Macromol.* **1992**, *25* (20), 5345–5352.
- (4) Yeh, T. F.; Reiser, A.; Dammel, R. R.; Pawlowski, G.; Roeschert, H. *Macromol.* **1993**, *26* (15), 3862–3869.
- (5) Hunek, B.; Cussler, E. *AIChE J.* **2003**, *48*, 661–672.
- (6) Tsiartas, P. C.; Flanagan, L. W.; Hinsberg, W. D.; Henderson, C. L.; Sanchez, I. C.; Bonnacaze, R. T.; Willson, C. G. *Macromol.* **1997**, *30*, 4656–4664.
- (7) Burns, S. D.; Schmid, G. M.; Tsiartas, P. C.; Willson, C. G.; Flanagan, L. *J. Vac. Sci. Technol. B* **2002**, *20* (2), 537–543.
- (8) Hinsberg, W.; Houle, F. A.; Lee, S. W.; Ito, H.; Kanazawa, K. *Macromol.* **2005**, *38* (5), 1882–1898.
- (9) Houle, F. A.; Hinsberg, W. D.; Sanchez, M. I. *Macromol.* **2002**, *35* (22), 8591–8600.

(10) Ito, H.; Wallraff, G. M.; Fender, N.; Brock, P. J.; Hinsberg, W. D.; Mahorowala, A.; Larson, C. E.; Truong, H. D.; Breyta, G.; Allen, R. D. *J. Vac. Sci. Technol. B* **2001**, *19* (6), 2678–2684.

(11) Ito, H.; Hinsberg, W. D.; Rhodes, L.; Chang, C. *Proceedings of the SPIE, Advances in Resist Technology and Processing XX* **2003**, 5039, 70–79.

(12) Prabhu, V. M.; Vogt, B. D.; Wu, W. L.; Douglas, J. F.; Lin, E. K.; Satija, S. K.; Goldfarb, D. L.; Ito, H. *Langmuir* **2005**, *21* (15), 6647–6651.

(13) Ito, H.; Allen, R. D.; Opitz, J.; Wallow, T. L.; Troung, H. D.; Hofer, D. C.; Varansai, P. R.; Jordhamo, G. M.; Jayaraman, S.; Vicari, R. *Proceedings of the SPIE, Advances in Resist Technology and Processing XVII* **2000**, 3999, 2–12.

(14) Houle, F. A.; Hinsberg, W. D.; Sanchez, M. I. *J. Vac. Sci. Technol. B* **2004**, *22* (2), 747–757.

(15) Houle, F. A.; Hinsberg, W. D.; Morrison, M.; Sanchez, M. I.; Wallraff, G.; Larson, C.; Hoffnagle, J. *J. Vac. Sci. Technol. B* **2000**, *18* (4), 1874–1885.

(16) Hinsberg, W. D.; Houle, F. A.; Sanchez, M. I.; Wallraff, G. M. *IBM J. Res. Dev.* **2001**, *45* (5), 667–682.

generator (PAG) within the photoresist film. At elevated temperature the photoacid diffuses and may catalyze hundreds of deprotection reactions^{15,19} by cleaving an acid-labile hydrophobic protecting group to yield a hydrophilic weakly acidic group. At short reaction times, the photoacid diffuses and reacts to a limited extent, leaving a distribution of nanometer-scale diffuse reaction domains²⁰ composed of hydrophilic groups within the initial hydrophobic continuum. In the case of long reaction times, the hydrophilic content pervades the film and the weak polyelectrolyte dissolves via reaction ionization–dissolution kinetics.⁸ In contrast to the behavior of thin films of statistical copolymers, the materials studied here have a locally heterogeneous composition due to the reaction–diffusion process.

Quartz crystal microbalance with energy dissipation and Fourier transform infrared spectroscopy measurements identify four regimes of film response for these unentangled polymer thin films when equilibrated with aqueous hydroxide solutions. As expected, fully protected polymer films do not swell due to their hydrophobic nature, and these films will dissolve in the aqueous developer solution when the polymer is fully deprotected. At intermediate reaction levels, the local morphology of the hydrophilic domain structure provides a physicochemical framework that permits film swelling and swelling with partial polymer dissolution. These measurements highlight factors that are crucial to comprehend the dissolution mechanism that controls the fidelity of imaged patterns.

II. Experimental Section

Certain commercial equipment and materials are identified in this paper in order to specify adequately the experimental procedure. In no case does such identification imply recommendations by the National Institute of Standards and Technology nor does it imply that the material or equipment identified is necessarily the best available for this purpose.

A. Materials. Poly(methyladamantyl methacrylate) (DuPont) with mass-average relative molecular mass of $M_{r,w} = 8800 \text{ g mol}^{-1}$ and polydispersity $M_{r,w}/M_{r,n} = 1.18$ was dissolved in cyclohexanone (Aldrich, Reagent Grade) at a concentration of 5% by mass. The photoacid generator triphenylsulfonium perfluorobutanesulfonate (TPS–PFBS) was added at a loading of 2% by mass of polymer. The mixture was then heated to 55 °C for 30 min to ensure complete dissolution of the polymer. Tetramethylammonium hydroxide solutions were prepared by diluting a 25% (by mass) stock solution (Aldrich) with deionized water purified and filtered by a Milli-Q system (Millipore) with final resistivity of 18 M Ω cm.

B. Sample Preparation. AT-cut quartz crystals (5 MHz, Q-Sense) coated with silicon oxide or chromium were treated with hexamethyldisilazane to improve the adhesion of the polymer films to the surface. Liquid hexamethyldisilazane was syringed upon the QCM crystals, heated for 90 s on a hot plate set at 150 °C, and, after cooling to room temperature, thoroughly rinsed with toluene (Aldrich, Reagent Grade). This procedure yielded hydrophobic surfaces having static water contact angles close to 90°. The polymer solution was then spin coated onto the QCM substrates at 209 rad/s (2000 rpm), followed by annealing at 130 °C for 60 s in a convection oven. The average film thickness was approximately 120 nm. The polymer-coated substrates were exposed to a broadband 248-nm filtered deuterium lamp (Oriel, 350 mW) for 30 s to generate the photoacid. The supported films were then baked at 90 °C for different periods

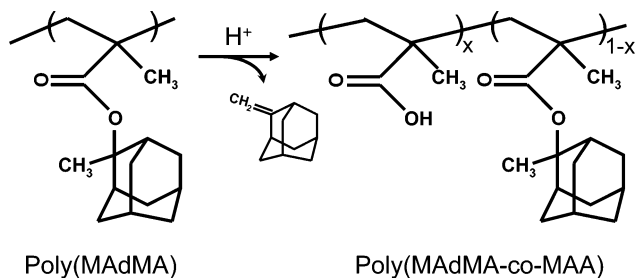


Figure 1. Acid-catalyzed deprotection products starting from homopolymer polymer to the copolymer of poly(methyladamantyl methacrylate-*co*-methacrylic acid). The average copolymer composition is determined quantitatively by reflectance infrared spectroscopy.

of time to obtain variable degrees of deprotection and then quenched to room temperature by placing the substrates on a large aluminum block. The deprotection reaction is an acid-catalyzed, thermally activated process that results in the adamantyl protecting group being removed to form a poly(methyladamantyl methacrylate-*co*-methacrylic acid) copolymer as shown in Figure 1.

C. FTIR Spectroscopy. The deprotection level (copolymer composition) and the amount of residual methylene adamantane in the films on the chromium-coated quartz crystals were measured by a Bruker Equinox 55 spectrometer (Billerica, MA) with a MCT detector in reflection mode. The VeeMax reflection optics is employed and is aligned to provide a 76° angle incidence. The entire setup is sealed into the sample compartment of the FTIR spectrometer using Plexiglas with a 10 mm sampling hole of the VeeMax system open to the atmosphere. A resolution of 4 cm^{-1} is used and 100 scans are averaged to improve the signal-to-noise ratio.

The quantification of deprotection reaction degree is based on the bending vibration mode of CH_3 (1360 cm^{-1}) in the MA group of PMAdMA. This band completely disappears and leaves a flat baseline if all the protected MA groups are reacted. The advantage of choosing this band to measure the deprotection level is that it not only gives an absolute value of deprotection reaction extent but also allows us to discriminate easily between the residual MA and the protected MA group. The quantification of the amount of residual MA is based on the stretching vibration of $\text{H}-\text{C}(=\text{C})$ (3065 cm^{-1}) in the free MA molecule. This band is isolated from other $\text{H}-\text{C}(-\text{C})$ vibration (usually $<3000 \text{ cm}^{-1}$), which makes it possible to quantify it accurately. Since a pure sample of MA is not available, the calibration from IR absorbance of MA to its molar quantity cannot be done directly. Instead, we use an indirect extrapolation method by assuming the MA is completely trapped if the deprotection level is close to zero. A quantitative relationship was determined to prepare films of known deprotection extents, based on the above UV exposure dose and bake temperature, such that the average level of methacrylic acid content (f_{MAA}) as a function of reaction time (t) was $f_{\text{MAA}} = 0.78(1 - e^{-0.05t})$.

D. Small-Angle Neutron Scattering: Polymer–Solvent Interaction Parameter. The Flory–Huggins interaction parameter (χ) between MAdMA segments and water was estimated from small-angle neutron scattering to be 8.7 in dimensionless units of $k_B T$ at 298 K, where k_B is the Boltzmann constant and T is temperature. Small-angle neutron scattering was performed on the NG 3 30 m instrument at the NIST Center for Neutron Research. The random phase approximation equations²¹ for polymer in solvent were fit to semidilute solutions of PMAdMA in deuterated tetrahydrofuran (THF) with statistical segment length and χ as the only fit parameters. Using the relationship between χ and the solubility parameter difference between components, which is known for protonated THF, the solubility parameter for MAdMA was determined.²² Therefore, χ for MAdMA–water was calculated using the known value of the solubility parameter for water.²² This methodology emphasizes that

(17) Schmid, G. M.; Stewart, M. D.; Singh, V. K.; Willson, C. G. *J. Vac. Sci. Technol. B* **2002**, *20* (1), 185–190.

(18) Houle, F. A.; Hinsberg, W. D.; Sanchez, M. I.; Hoffnagle, J. A. *J. Vac. Sci. Technol. B* **2002**, *20* (3), 924–931.

(19) Mckean, D. R.; Schaedel, U.; Macdonald, S. A. *J. Polym. Sci. Part A* **1989**, *27* (12), 3927–3935.

(20) Jones, R. L.; Hu, T. J.; Lin, E. K.; Wu, W. L.; Goldfarb, D. L.; Angelopoulos, M.; Trinquet, B. C.; Schmid, G. M.; Stewart, M. D.; Willson, C. G. *J. Polym. Sci. Part B* **2004**, *42* (17), 3063–3069.

(21) Hammouda, B. *Adv. Polym. Sci.* **1993**, *106*, 87–133.

(22) *Polymer Handbook*, 4 ed.; Wiley-Interscience: New York, 1999; Vol. 2, p 675.

a large chemical mismatch exists between the PMAdMA segments and aqueous solutions.

E. Quartz Crystal Microbalance Technique. The response of the thin films to varied concentrations of TMAH solutions was measured by a quartz crystal microbalance (Q-Sense) with dissipation mode (QCM-D). The QCM-D setup follows the changes in the resonance frequency (≈ 5 MHz) as well as the overtones (15, 25, and 35 MHz) of the polymer-coated quartz crystal. After mounting the quartz crystals onto the temperature-controlled QCM flow cell (maintained at 298 K), the polymer films were equilibrated for 5 min in deionized water. The liquid flow rate was adjusted to 1.025 mL/min. During this equilibration stage, changes in the crystal response can be attributed to viscosity and density effects from the water²³ with negligible water absorption into the film. After equilibrating the polymer film in water, liquid flow was switched to introduce aqueous TMAH solutions into the cell. Changes in the resonance frequency as well as energy dissipation of the polymer-coated quartz crystals upon exposure to TMAH solutions were then measured as a function of time. The shifts in the resonance frequency as well as energy dissipation were calculated relative to the resonance frequency and energy dissipation of the coated crystal when immersed in water. For the polymer films used in this study, we were unable to accurately measure the shifts in the overtone frequencies due to the rapid kinetics and large dissipative losses in highly swollen films. Therefore, only changes in the fundamental frequency of the quartz and the energy dissipation at this frequency will be presented; uncertainties are calculated as the estimated standard deviation from the mean. In the case where the limits are smaller than the plotted symbols, the limits are left out for clarity.

The QCM technique²⁴ monitors the change in the mass of an oscillating quartz crystal. In a vacuum, the change in mass (Δm) of a rigid film coated onto the surface of the quartz crystal causes a shift in resonance frequency ($\Delta F = F_0 - F$) that can be calculated using the Sauerbrey relationship

$$\Delta F = -\frac{F_0}{\rho_q h_q} \Delta m \quad (1)$$

where F_0 is the fundamental resonance frequency of the quartz crystal and ρ_q and h_q are the density and thickness of the quartz crystal. However, if the coated film is viscoelastic in nature and is immersed in a liquid, the change in the resonance frequency is given by²⁴

$$\Delta F \approx -\frac{1}{2\pi\rho_q h_q} \left(\frac{\eta_1}{\delta_1} + h_1 \rho_1 \omega - 2h_1 \left(\frac{\eta_1}{\delta_1} \right)^2 \frac{\eta_1 \omega^2}{\mu_1^2 + \omega^2 \eta_1^2} \right) \quad (2)$$

where $\omega = 2\pi F$, $\delta_1 = \sqrt{\eta_1/\rho_1\omega}$, h_1 is the thickness of the viscoelastic film; μ_1 is the elastic shear modulus of the viscoelastic film, and η_1 and ρ_1 are the shear viscosities of the liquid and viscoelastic film, respectively. The viscoelastic nature of the coated over layer also results in a viscous loss (dissipation) within the film, which is given by²⁴

$$\Delta D \approx \frac{1}{\omega\rho_q h_q} \left(\frac{\eta_1}{\delta_1} + 2h_1 \left(\frac{\eta_1}{\delta_1} \right)^2 \frac{\mu_1 \omega}{\mu_1^2 + \omega^2 \eta_1^2} \right) \quad (3)$$

For such a film, determination of the film thickness requires the simultaneous measurement of the shift in the resonance frequency as well as the energy dissipation.^{25,26} One can then use eqs 2 and 3 to determine the thickness as well as the viscoelastic properties of the film. However, since there are four independent variables (ρ , μ , η , and h) involved in the above equations, an accurate estimation of the material parameters requires the measurement of ΔF and ΔD

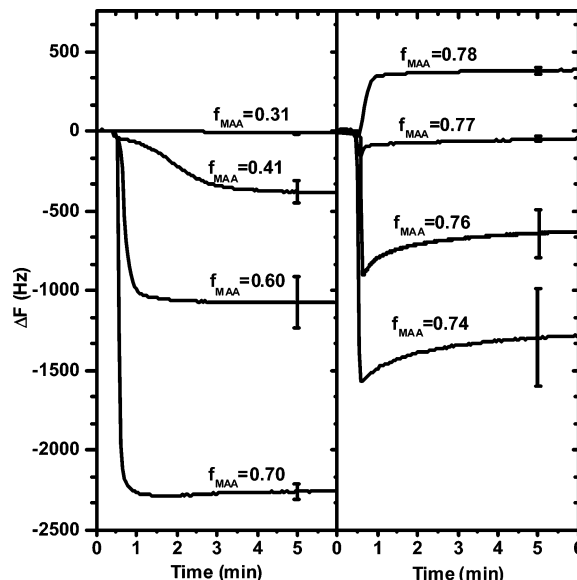


Figure 2. Change in QCM frequency (ΔF) after exposure to 0.065 N tetramethylammonium hydroxide solution for different average methacrylic acid copolymer content (f_{MAA}).

for the fundamental resonance frequency, as well as the harmonic overtones of the fundamental frequency.

III. Results

Polymer thin films with different average methacrylic acid (f_{MAA}) concentrations were prepared by the in situ acid-catalyzed deprotection reaction,²⁷ where the hydrophobic PMAdMA is converted into a methacrylic acid containing copolymer, as shown in Figure 1. The photoacid reaction—diffusion kinetics depends on UV exposure dose and photoacid generator (PAG) loading, which define the acid concentration, as well as photoacid chemistry and size, which determine the acidity and diffusivity.^{15,16,18,28–31} To avoid complications from these factors, a constant photoacid concentration is maintained by complete photolysis of a dilute PAG concentration by UV exposure.³¹ A systematic variation of deprotection is produced by changing the reaction time. This approach results in thin films with a morphology in chemical composition induced by photoacid deprotection in contrast with films prepared from statistical copolymers.

The response of these films to water and aqueous hydroxide solutions was characterized by the time dependence of the QCM-D signal. In Figure 2, the change in resonance frequency (ΔF) upon exposure to a 0.065 N TMAH solution is shown versus equilibration time for an average f_{MAA} ranging from 0 to 0.78 mole fraction. The corresponding change in energy dissipation (ΔD) by the polymer film is shown in Figure 3. Qualitatively, a drop in the resonance frequency may be interpreted as film swelling, while an increase in the resonance frequency indicates film dissolution. Similarly, an increase in the dissipation can be interpreted as being representative of viscous losses due to the swollen film.

(27) Kang, S. H.; Prabhu, V. M.; Vogt, B. D.; Lin, E. K.; Wu, W. I.; Turnquest, K. *Polymer* **2006**, *47* (18), 6293–6302.

(28) Stewart, M. D.; Tran, H. V.; Schmid, G. M.; Stachowiak, T. B.; Becker, D. J.; Willson, C. G. *J. Vac. Sci. Technol. B* **2002**, *20* (6), 2946–2952.

(29) Ablaza, S. L.; Cameron, J. F.; Xu, G. Y.; Yueh, W. *J. Vac. Sci. Technol. B* **2000**, *18* (5), 2543–2550.

(30) Stewart, M. D.; Somervell, M. H.; Tran, H. V.; Postnikov, S. V.; Willson, C. G. *Proc. SPIE* **2000**, *3999*, 665–674.

(31) Wallraff, G.; Hutchinson, J.; Hinsberg, W.; Houle, F.; Seidel, P.; Johnson, R.; Oldham, W. *J. Vac. Sci. Technol. B* **1994**, *12* (6), 3857–3862.

(23) Kanazawa, K. K.; Gordon, J. G. *Anal. Chim. Acta* **1985**, *175*, 99–105.

(24) Voinova, M. V.; Rodahl, M.; Jonson, M.; Kasemo, B. *Phys. Scr.* **1999**, *59* (5), 391–396.

(25) Kanazawa, K. K. *Faraday Discuss.* **1997**, (107), 77–90.

(26) White, C. C.; Schrag, J. L. *J. Chem. Phys.* **1999**, *111* (24), 11192–11206.

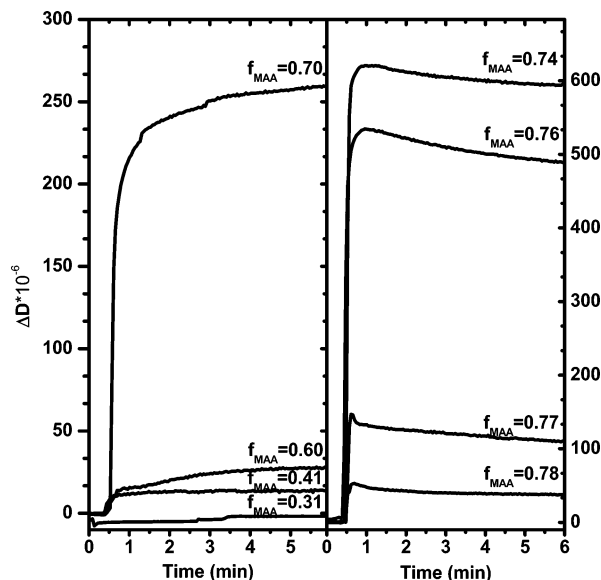


Figure 3. Change in QCM energy dissipation (ΔD) after exposure to 0.065 N tetramethylammonium hydroxide solution for different average methacrylic acid copolymer content (f_{MAA}).

The lowest f_{MAA} investigated were 0 and 0.31, in which no measurable mass uptake was observed upon exposure to pure water or TMAH. From Figure 2, once the f_{MAA} is increased to 0.41, swelling occurs as evidenced by the decrease in the quartz oscillation frequency and the kinetics of swelling plateaus within minutes. There is no further change in frequency for times as long as 45 min. Hence, we refer to these stable films as being in a quasiequilibrium state. The short-time behavior is shown to highlight the time scale of the film response. As the average f_{MAA} is increased to 0.60, the response to the hydroxide solution has faster kinetics as well as a larger frequency change that is indicative of increased film swelling. The same trend is observed for $f_{\text{MAA}} = 0.70$. However, we notice that, with enhanced film swelling, there is a slight recovery in ΔF leading to a shallow minimum followed by a plateau. This effect is amplified as the average MAA content increases, as seen from the right-hand side of Figure 2 for $f_{\text{MAA}} = 0.74, 0.76,$ and 0.77 . The film response is to first swell and then exhibit a form of relaxation leading to a positive change in ΔF , consistent with partial dissolution of the film. This preswelling followed by dissolution provides evidence for a clear transition in film behavior as a function of the average film composition and processing conditions. However, in these cases, the plateau response indicates that the polymer remains in a swollen quasiequilibrium condition. Note that for $f_{\text{MAA}} = 0.74, 0.76,$ and 0.77 , the dissipation of these films at quasiequilibrium is still significant, corresponding to a highly swollen structure. An overall positive change in ΔF due to significant mass loss is observed only at the highest $f_{\text{MAA}} = 0.78$.

The energy dissipation measured in the QCM measurement qualitatively tracks the mechanical response of the film. At the lowest $f_{\text{MAA}} = 0.31$, where no swelling is observed, the energy dissipation is near zero, indicating an elastic film where the Sauerbrey expression can be used to quantify film thickness.^{8,32,33} However, as the film swells, the energy dissipated increases, reaching a level of 265×10^{-6} for $f_{\text{MAA}} = 0.70$. Therefore, the films with the largest change in frequency (most swollen) display a measurable viscous response. As the f_{MAA} increases, the ΔD

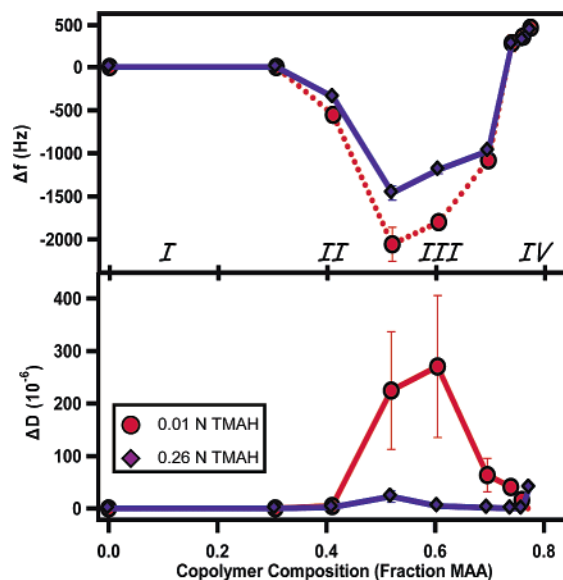


Figure 4. Polyelectrolyte quasiequilibrium phase behavior determined from the long-time QCM response in frequency (ΔF) and dissipation (ΔD). Four regimes are observed: (I) nonswelling films ($0 < f_{\text{MAA}} \leq 0.3$), (II) swelling without dissolution ($0.3 < f_{\text{MAA}} \leq 0.5$), (III) swelling accompanied by partial film dissolution ($0.5 < f_{\text{MAA}} \leq 0.7$), and (IV) film dissolution with residual adsorbed layer ($f_{\text{MAA}} > 0.7$). Lines serve as a guide for the eye.

exhibits a maximum with time, followed by a recovery and plateau to 600×10^{-6} and 500×10^{-6} for $f_{\text{MAA}} = 0.74$ and 0.76 , respectively, consistent with the changes in frequency. The films at quasiequilibrium behave more elasticlike at higher f_{MAA} (0.77 and 0.78) with a significant decrease in ΔD in comparison to films with only slightly less MAA content. These data illustrated in Figures 2 and 3 correspond to the film's response to 0.065 N TMAH. Changing the base concentration influences the swelling–dissolution response of these films. Figure 4 illustrates the quasiequilibrium ΔF and ΔD for films swollen by 0.01 and 0.26 N TMAH. There is no significant shift in the type of response for different f_{MAA} ; only the magnitude of the swelling is influenced by the TMAH concentration.

IV. Discussion

The poly(methyladamantyl methacrylate) homopolymer is hydrophobic as judged by its static water contact angle of 78° , large chemical mismatch between MADMA and water quantified by the Flory–Huggins interaction parameter ($\chi = 8.7$), and lack of water or hydroxide solution uptake. However, the acid-catalyzed deprotection reaction of this polymer into a copolymer of poly(methyladamantyl methacrylate-*co*-methacrylic acid) introduces hydrophilic character to the polymer, leading to a large change in physicochemical properties of the polymer film when it is immersed in aqueous alkaline solutions. The range of swelling and dissolution behavior is controlled by the average film composition and spatial distribution of hydrophilic and hydrophobic groups induced by the in situ reaction (Figure 1).

A. Phase Behavior. The plateau in the QCM response with time can be used to quantify the long-time quasiequilibrium behavior of the swelling of the polymer thin film. The plateau values in ΔF and ΔD are plotted separately in Figure 4 for two additional TMAH concentrations, 0.01 and 0.26 N. For clarity, the 0.065 N data are not included. From inspection of the QCM-D data and the form of the kinetic curves, we observe four distinct regimes of behavior as a function of average film composition. In regime I there is no film swelling between compositions (0

(32) Lee, S. W.; Hinsberg, W. D.; Kanazawa, K. *Anal. Chem.* **2002**, *74* (1), 125–131.

(33) Vogt, B. D.; Lin, E. K.; Wu, W. L.; White, C. C. *J. Phys. Chem. B* **2004**, *108* (34), 12685–12690.

$< f_{\text{MAA}} < 0.3$); at higher average degrees of protection ($0.3 < f_{\text{MAA}} < 0.5$), regime II is characterized by film swelling only; in regime III ($0.5 < f_{\text{MAA}} < 0.7$), partial dissolution of a swollen film is observed; and finally, in regime IV ($f_{\text{MAA}} > 0.7$), nearly complete dissolution is observed.

The different responses of the films to the aqueous solution are a function of the copolymer composition and the distribution of the methacrylic acid within the polymer films. These methacrylic acid groups are generated through an in situ reaction involving the cleavage of adamantyl side groups. Consequently, the methacrylic acid distribution within the films will be dependent on the amount of photoacid generated within the film as well as the ability of the photoacid to diffuse and react. At the UV exposure conditions employed, all the photoacid generator molecules present in the film are activated for subsequent reaction and diffusion. At short reaction bake times, the photoacid diffuses and reacts to a limited extent, forming domains of reacted photoresist that do not overlap.²⁰ Therefore, under these conditions the polymer film may be regarded as a hydrophobic continuum with a distribution of reacted domains composed of hydrophilic methacrylic acid groups. Since the deprotection domains may span several different chains, the average film composition does not correspond to the composition of any particular chain. In the low-reaction-extent regimes, we expect the domains to be nonoverlapping, in concert with earlier investigations. At this early stage, regime I, the hydrophobic continuum of protected polymer prevents penetration of water. The methacrylic acid content is inaccessible to the solution. As observed in Figure 4, no swelling is observed at $f_{\text{MAA}} \approx 0.3$ and is independent of water and base concentration, supporting this concept of inaccessible hydrophilic regions for the solution molecules.

With longer reaction time, diffusion and reaction of the photoacid molecules increase the methacrylic acid content, which eventually forms a connected or percolated network. The percolated character of these groups provides pathways for solute transport throughout the film, enabling the hydroxide ions to induce film swelling by titrating the methacrylic acid groups.^{34–36} The onset of film swelling in our system corresponds to an average methacrylic acid fraction greater than $f_{\text{MAA}} = 0.3$, a value close to that predicted for the percolation threshold on a simple cubic lattice ($p_c = 0.3116$). Above this percolation threshold in methacrylic acid content, the rate of swelling increases, as shown in Figure 2, as does the magnitude of the frequency shift corresponding to uptake of the solution. The film swelling is enabled by the percolated distribution of deprotection domains, while the degree of swelling is controlled by the ionizable group content.

The swollen nature of the copolymer film is consistent with the energy dissipation in regime II and the large changes in the values of ΔF . These data raise an interesting question about the origin of the stability of the swollen films. For most polymer gels, film stability during swelling is due to the existence of cross-link junctions formed covalently or by physical entanglement of high molecular weight chains.³⁷ However, the system here does not have any chemical cross-linking and the molecular weight of the polymers is below the entanglement molecular weight. The stability of our swollen films is attributed to physicochemical junctions formed by the continuum of hydro-

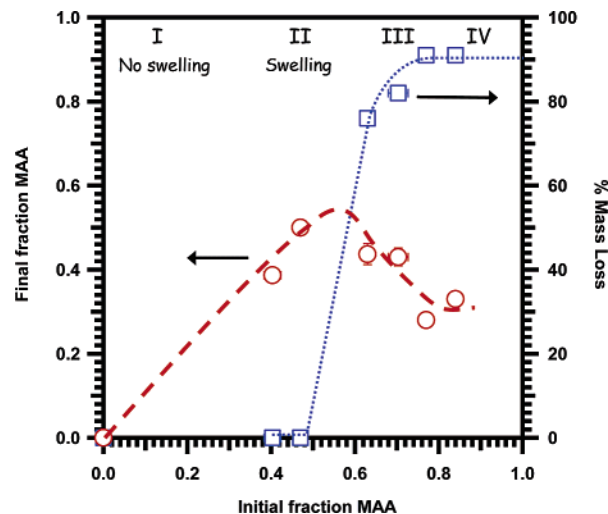


Figure 5. FTIR measurements of the change in the film composition and mass before and after film exposure to 0.26 N TMAH. In the nonswelling and swelling-only regime, no mass loss and remarkably no change in composition are measured, as predicted by the QCM response. In regimes III and IV, a larger hydrophobic content is directly measured due to partial dissolution of MAA-rich polyelectrolyte chains through the percolative network.

phobic (methyladamantyl) groups. The formation of these junctions is analogous to the aggregation of hydrophobic/hydrophilic copolymers in aqueous solution.³⁸ The ability of the film to sustain the swelling implies that the concentration or distribution of the hydrophobic domains also is above the percolation threshold. Therefore, the generality of these results should depend on the relative hydrophobicity of the protected to deprotected functional groups.

Further, the observations of swelling will reduce the polymer concentration near the solid substrate. One consequence is that the film may partially detach or delaminate during the measurement. This problem is solved by the hexamethyldisilazane (adhesion promoter) surface treatment. However, if partial detachment were to occur, water would accumulate at the substrate, thus lowering the average viscosity of the thin film overlayer, leading to an increase in ΔD from the initial elastic film in contact with water. Simultaneously, a positive ΔF shift would result, due to less film mass coupled with the QCM oscillator. As the kinetics of detachment progresses, the dissipation shift would go through a maximum and return to the initial ΔD due to only water coupled to the QCM oscillator, while a monotonic positive shift in ΔF would be observed. The present experiments do not show these signatures of physical detachment nor delamination, as assured by the ΔD and ΔF responses. Moreover, independent FTIR measurements quantifying mass loss confirm these results.

Following on to regime III, the drop in plateau values of ΔF in Figure 4 as the methacrylic acid fraction exceeds 0.5 is due to the partial dissolution of the polyelectrolyte chains from the swollen layer. This observation was confirmed independently by FTIR measurements. In Figure 5, the final MAA composition (left-hand axis) and the total mass loss (right-hand axis) of the developed film are plotted versus the initial composition for films dissolved in 0.26 N TMAH. In regimes I and II, as expected, there is no change in methacrylic acid content, nor any mass loss as determined by FTIR. After quantifying the change in average film composition, swelling in regime III expels only a fraction of the chains composed of high levels of MAA, leading to a reduced average MAA content.

(34) Kumacheva, E.; Rharbi, Y.; Winnik, M. A.; Guo, L.; Tam, K. C.; Jenkins, R. D. *Langmuir* **1997**, *13* (2), 182–186.

(35) Annable, T.; Buscall, R.; Ettelaie, R.; Whittlestone, D. *J. Rheol.* **1993**, *37* (4), 695–726.

(36) Petit, F.; Lliopoulos, I.; Audebert, R. *J. Chim. Phys. Phys.-Chim. Biol.* **1996**, *93* (5), 887–898.

(37) Flory, P. *Phase Equilibria*. In *Principles of Polymer Chemistry*; Cornell University Press: Ithaca, NY, 1953; p 577.

(38) Noda, T.; Morishima, Y. *Macromol.* **1999**, *32* (14), 4631–4640.

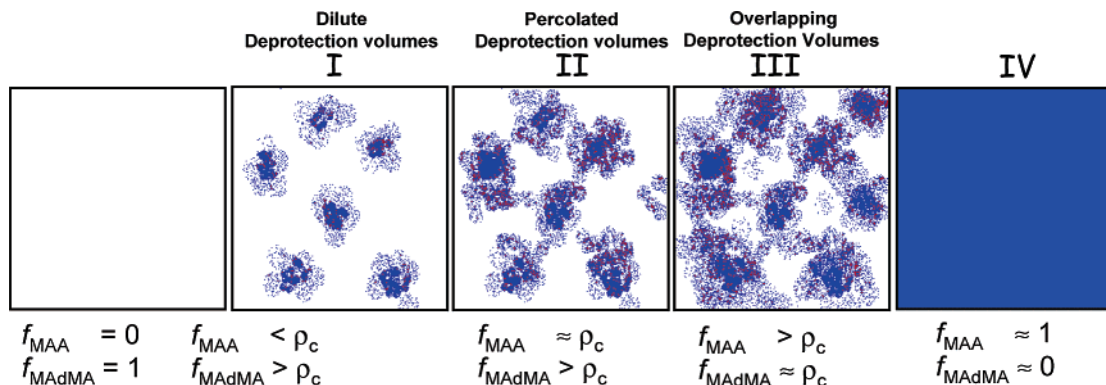


Figure 6. Schematic of the deprotection morphologies of the four regimes and relationship to the average f_{MAA} (and f_{MAdMA}) and percolation threshold (ρ_c).

This behavior shows that the change in solubility of the polymer films occurs gradually and dissolution proceeds via the expulsion of highly charged polymer chains from a swollen matrix. The number of chains expelled from the matrix increases with increasing methacrylic acid content. These observations can be interpreted with respect to the spatial heterogeneity in the local copolymer composition induced by the reaction–diffusion process as follows: as the average MAA fraction of the copolymer film increases, chains with excess methacrylic acid contents are rendered soluble and escape the swollen matrix (regime III in Figure 4) on a time scale associated with the relaxation of the matrix or disengagement of the chain from the film. As the average methacrylic acid content increases, the relative fraction of soluble chains increases, at the expense of the hydrophobic matrix. Therefore, the film dissolves faster than it swells, which corresponds to regime IV in Figure 4. This phenomenon is seen in the kinetic data plotted in Figure 2. This hypothesis of polymer chains dissolving from a matrix (regime III) is confirmed by FTIR measurements of the change in the average methacrylic acid content as well as the change in the total film mass after exposure to a 0.26 N TMAH solution (Figure 5). A schematic of the morphology expected from these regimes is summarized by Figure 6. Beginning with a completely protected PMAAdMA film, photoacids deprotect local regions of the polymer. Initially, these can be envisioned as isolated fuzzy blobs²⁰ (regime I). As the deprotection continues, the deprotection volumes begin to overlap, forming a percolated network (regime II), which allows the film to swell. In regime III, this overlap grows, but a network of the hydrophobic PMAAdMA remains, preventing complete dissolution. At high deprotection (regime IV), the hydrophobic domains are no longer percolated, leading to nearly complete dissolution. The hydrophilic domains and their percolation are governed by the average composition with respect to the percolation threshold. Most experimental data involving photoresist polymer dissolution correspond to regime IV, where the deprotection morphology was not considered.

In regime IV, reflectance IR as well as QCM measurements indicate that the polymer film does not fully dissolve upon exposure to TMAH solutions. From the IR measurements, it appears that the residual layer corresponds to approximately 10–15% of the original film mass and has an average methacrylic acid composition that is close to the percolation threshold for film swelling. The low values of ΔD for this residual layer also confirm its relatively unswollen nature. The origin of this residual layer is not clear and deserves further study.

B. Regime II: Hydroxide Concentration Effect. Figure 4 highlights the effect of TMAH concentration on the extent of film swelling within regime II. The data in Figure 4 demonstrate that the swelling of the films is larger in the more dilute TMAH

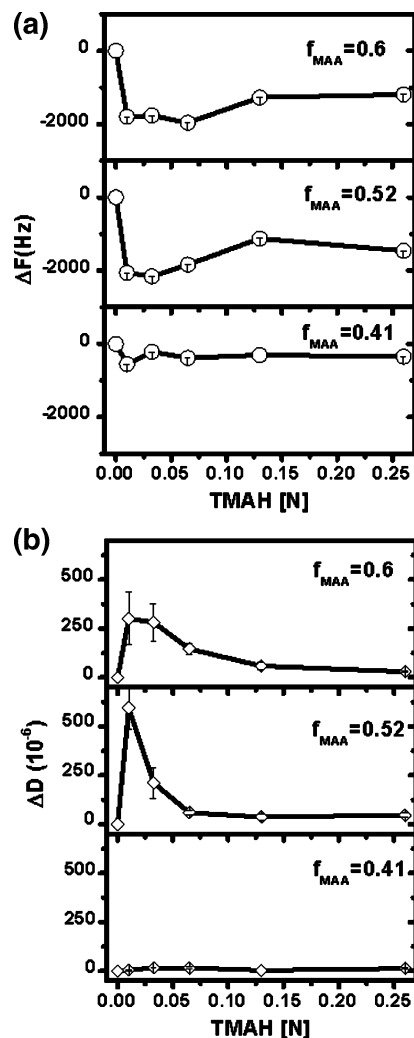


Figure 7. Change in (a) frequency (ΔF) and (b) energy dissipation (ΔD) for three average methacrylic acid composition, within the quasiequilibrium swelling regime, as a function of TMAH concentration.

solution. To obtain a better understanding of this phenomenon, we studied three different copolymer compositions with methacrylic acid fraction ranging from 0.4 to 0.6 as a function of TMAH concentration. The changes in ΔF and ΔD of these films upon equilibration are plotted in parts a and b, respectively, of Figure 7. In the case of copolymer films containing 40% methacrylic acid, ΔF and ΔD exhibit a weak dependence on TMAH concentration, indicating that the extent of film swelling at this composition does not depend strongly upon the hydroxide

concentration. However, as the average methacrylic acid content of the film increases to 52 and 60% MAA, the dependence of ΔF and ΔD on hydroxide concentration becomes more pronounced. Most noticeable, ΔD decreases sharply with increasing TMAH concentration after increasing substantially from pure water. The in situ titration of the methacrylic acid groups (pK_a of 7.2) by TMAH is the primary source for the film swelling. At 0.01 N TMAH, the polymer films are completely ionized. Increasing the TMAH concentration results in electrostatic repulsions within the film and is followed by the increased osmotic pressure by the TMA^+ counterions, leading to a decrease in swelling. Since $\Delta D \sim h\mu^{-1}\eta^{-2}$, a drop in dissipation with increasing TMAH concentration may be interpreted as an increase in shear viscosity (η), an increase in shear modulus (μ), a decrease in film thickness, or a combination thereof, consistent with a lower extent of film swelling.

Increasing the TMAH concentration leads to a diffusion of excess TMAH into the polymer film, resulting in screening of the electrostatic repulsion between the ionized groups of the polymer chains as well as reduced osmotic driving force for swelling.³⁷ This would be expected by true cross-linked gel behavior, as observed by Horkay et al. on model charged gels where an increased electrolyte concentration results in a decreased swelling ratio.³⁹ In the current case, excess TMAH will contribute to the solution ionic strength. This reduced swelling extent will increase in the local polymer concentration, thereby increasing the shear viscosity and elastic storage modulus. This behavior is consistent with the decrease in ΔD such as those observed in Figure 7b.

While the direct comparison to a quantitative theory is currently lacking, one important element that controls the response of the polymer films to an aqueous base solution is the effective physical cross-link density from the hydrophobic matrix. This response strongly depends on the fractal or percolation structure of weakly charged groups that would render the chains soluble in the absence of the hydrophobic domains. These charged domains undergo ionization, causing film swelling, but also induce measurable changes in the mechanical properties. Additional experiments that tune the degree of chemical mismatch (hydrophobicity) as

well as introduce well-defined morphologies (deprotection) such as that examined by colloidal templating⁴⁰ are needed to quantify the effects of different parameters on this important technological problem.

V. Conclusion

The behavior of these thin polymer films upon exposure to aqueous base solution is controlled by an in situ prepared copolymer structure. The onset of film swelling is consistent with a percolation framework; when the weakly acidic methacrylic acid fraction exceeds 0.3, these films swell. The swollen films are stable, suggestive of a quasiequilibrium state, due to the balance between the uptake of solvent into the film and the spatial extent of physical cross-links from the distribution of the hydrophobic domains in the polymer matrix. The effect of hydroxide concentration did not change the onset to regime II (swelling only), consistent with the need for a percolation pathway of hydrophilic groups before any swelling can occur. However, within regime II, in the extent of film swelling was controlled by the hydroxide concentration, with greatest swelling observed at low TMAH concentration. Regime III exhibits partial dissolution of highly charged polyelectrolyte chains. The chains that do not yet have sufficient hydrophilicity are trapped by the hydrophobic copolymer structure, as determined by FTIR. This behavior highlights the coupling of the diffusion of hydroxide and solvent into the film, inducing ionization and providing a sufficient thermodynamic driving force for the chains to escape the interconnected structure. These results are different from those for previous generations of photoresists, where swelling was not an important factor and surface ionization was the rate-limiting step for dissolution. The development of a predictive model requires a minimum of including the spatial extent of chemical heterogeneity to recover these observations on unentangled weakly acidic polyelectrolyte films.

Acknowledgment. This work was supported by SEMATECH under Agreement #309841 OF. The authors acknowledge Dr. William Hinsberg (IBM Almaden Research Center) for helpful technical discussions, Dr. Curtis Meuse (Biochemical Science Division, NIST) for assistance in the reflection IR measurements, and Drs. Jim Sounik and Michael Sheehan (DuPont Electronic Polymers) for providing the polymers used in this study.

LA061773P

(39) Horkay, F.; Tasaki, I.; Bassler, P. J. *Biomacromolecules* **2000**, *1* (1), 84–90.

(40) Liu, L.; Li, P. S.; Asher, S. A. *Nature (London)* **1999**, *397* (6715), 141–144.